THE JOURNAL OF BIOLOGICAL CHEMISTRY VOL. 283, NO. 13, pp. 8756–8764, March 28, 2008

Kv1.5 Association Modifies Kv1.3 Traffic and Membrane Localization*[S]

Received for publication, October 3, 2007, and in revised form, January 14, 2008 Published, JBC Papers in Press, January 24, 2008, DOI 10.1074/jbc.M708223200

Rubén Vicente[‡1], **Núria Villalonga**[‡1], **Maria Calvo**[§], **Artur Escalada**[¶1], **Carles Solsona**[¶], **Concepció Soler**[¶], **Michael M. Tamkun**[‖2], **and Antonio Felipe**[‡2,3]

From the [‡]*Molecular Physiology Laboratory, Departament de Bioquímica i Biologia Molecular, Institut de Biomedicina, Universitat de Barcelona, Avenida Diagonal 645, E-08028 Barcelona, Spain, the* [§]*Departament de Biologia Cellular, Institut d'Investigacions Biomèdiques August Pi i Sunyer, Universitat de Barcelona, 08036 Barcelona, Spain, the* [¶]*Departament de Patologia i Terapèutica Experimental, Universitat de Barcelona-Campus de Bellvitge, E-08907 Hospitalet de Llobregat, Spain, and the* [‖]*Department of Biomedical Sciences, Colorado State University, Fort Collins, Colorado 80523*

Kv1.3 activity is determined by raft association. In addition to Kv1.3, leukocytes also express Kv1.5, and both channels control physiological responses. Because the oligomeric composition may modify the channel targeting to the membrane, we investigated heterotetrameric Kv1.3/Kv1.5 channel traffic and targeting in HEK cells. Kv1.3 and Kv1.5 generate multiple heterotetramers with differential surface expression according to the subunit composition. FRET analysis and pharmacology confirm the presence of functional hybrid channels. Raft association was evaluated by cholesterol depletion, caveolae colocalization, and lateral diffusion at the cell surface. Immunoprecipitation showed that both Kv1.3 and heteromeric channels associate with caveolar raft domains. However, homomeric Kv1.3 channels showed higher association with caveolin traffic. Moreover, FRAP analysis revealed higher mobility for hybrid Kv1.3/Kv1.5 than Kv1.3 homotetramers, suggesting that heteromers target to distinct surface microdomains. Studies with lipopolysaccharide-activated macrophages further supported that different physiological mechanisms govern Kv1.3 and Kv1.5 targeting to rafts. Our results implicate the traffic and localization of Kv1.3/Kv1.5 heteromers in the complex regulation of immune system cells.

The voltage-gated (Kv)[4] Kv1.3 channel is involved in the maintenance of the resting membrane potential in immune system cells. This protein plays a critical role during activation and proliferation of leukocytes, and several studies point to this channel as an excellent target for immunomodulation (1, 2). Kv1.3 is abundantly expressed on so-called "T-effector memory cells." These T-cells are key mediators in autoimmune inflammatory diseases. Kv1.3 blockers show more specificity for autoreactive T-effector memory cells than any molecular target expressed on all T-cells. In fact, Kv1.3 inhibitors ameliorate the symptoms of several T-cell-mediated diseases. In addition to the level of Kv expression, the proper plasma membrane localization and protein partnerships are critical for the regulation of channel steady state properties (1, 2). Therefore, the identification of the components of the channel complex and their regulation are essential for their possible use in pharmacology.

Kv channel expression in leukocytes is controlled post-translationally. Thus, Kv1.3 activity could be regulated by kinases, modulatory β subunits, and assemblies of other *Shaker* (Kv1) isoforms. Although considerable progress has been made in the first two subjects, less is known about the heterotetrameric structure of the functional channel (3–7). The Kv subunit composition determines the activity and the pharmacology of the channel and affects surface expression and membrane localization (8, 9). Kv1.3 coassembles with Kv1.1, Kv1.2, and Kv1.4 in the brain (10, 11) and forms heterotetrameric structures with Kv1.5 in macrophages (12, 13). Hybrid channels express distinct biophysical and pharmacological properties, and the Kv1.3/Kv1.5 ratio is modulated by cytokines leading to different phenotypes (12).

Recently, there has been interest in the channel targeting to the membrane that defines the protein microenvironment. Membrane microdomains rich in cholesterol and sphingolipids, called lipid rafts, work as platforms on which signal transduction pathways interface (14). Multiple Kv channels have affinity for lipid rafts, and different isoforms target to distinct lipid microdomains (15). In this context, Kv1.3 targets to raft domains involved in immunological synapses in T-cells (16). Furthermore, channel activity is regulated by the composition of the lipid raft (17, 18).

* This work was supported by Ministerio de Educación y Ciencia Grants BFI2002-00764 and BFU2005-00695 (to A. F.) and SAF2005-00736 and BFU2006-06076 (to C. S.) and National Institutes of Health Grants HL49330 and NS41542 (to M. M. T.). The costs of publication of this article were defrayed in part by the payment of page charges. This article must therefore be hereby marked "*advertisement*" in accordance with 18 U.S.C. Section 1734 solely to indicate this fact.

[S] The on-line version of this article (available at http://www.jbc.org) contains supplemental Fig. S1 and Movies S1–S4.

[1] Recipients of fellowships from the Universitat de Barcelona, the Ministerio de Educación y Ciencia, and the Fundació Marató TV3.

[2] Both authors contributed equally to this work.

[3] To whom correspondence should be addressed: Molecular Physiology Laboratory, Departament de Bioquímica i Biologia Molecular, Universitat de Barcelona, Avda. Diagonal 645, E-08028 Barcelona, Spain. Tel.: 34-934034616; Fax: 34-934021559; E-mail: afelipe@ub.edu.

[4] The abbreviations used are: Kv, voltage-gated potassium channel; ER, endoplasmic reticulum; FRAP, fluorescence recovery after photobleaching; FRET, fluorescence resonance energy transfer; LPS, lipopolysaccharide; MβCD, methyl-β-cyclodextrin; PBS, phosphate-buffered saline; CHAPS, 3-[(3-cholamidopropyl)dimethylammonio]-1-propanesulfonic acid; Mes, 4-morpholineethanesulfonic acid; YFP, yellow fluorescent protein; PKC, protein kinase C; PKA, cAMP-dependent protein kinase; CFP, cyan fluorescent protein.

In this study, we focus on changes in traffic and targeting of Kv1.3 by heteromultimeric association with Kv1.5. Both channels are present in mononuclear phagocytes, such as macrophages and dendritic cells (12, 13, 19–21). Activated macrophages are present in sites during inflammation. They produce cytokines and act as antigen-presenting cells establishing immunological synapses with T-cells. Kv1.3 activity determines the level of the macrophage activation, and this is conditioned by the presence of Kv1.5 (12, 13, 19, 22). Kv1.3 and Kv1.5 coassemble as heteromultimeric complexes, and the oligomeric stoichiometry compromises pharmacological responses (13). Although therapies that selectively suppress T-effector memory cells without affecting other lymphoid subsets would have immense value, the beneficial effects of Kv1.3 antagonists might be in part due to their inhibitory action on macrophages. However, Kv channel redundancy may allow these cells to escape the inhibitory effects of actual Kv1.3 blockers (13). Therefore, a deeper understanding of the functional complex is needed to warrant the development of more specific Kv1.3 blockers for autoimmune disease therapies.

Interestingly, both proteins have been located in raft microdomains, and their functions can be influenced by lipid-protein interactions (17, 23, 24). We report that functional Kv1.3/Kv1.5 heterotetrameric channels exhibit different location and targeting. In contrast to Kv1.5, Kv1.3 traffics efficiently to the membrane, and the heterotetramer composition determines the subcellular distribution. We suggest that Kv1.3 and the hybrid Kv1.3/Kv1.5 target to different lipid raft populations. Our data have physiological relevance because experiments on macrophages indicate that the expression of heteromeric Kv1.5-containing channels impairs their localization in rafts. However, LPS-induced activation, which selectively increases the number of Kv1.3 subunits in the heterotetramer (12, 13, 19), led to a relocalization of Kv1.3/Kv1.5 channels in lipid rafts. In summary, the presence of Kv1.5 modifies the channel targeting to raft membrane microdomains. Thus, different membrane platform locations must be contemplated as an important regulatory mechanism of Kv1.3 in leukocyte physiology.

EXPERIMENTAL PROCEDURES

Expression Plasmids, Cell Culture, and Transient Transfections—Rat Kv1.3 in pRcCMV was provided by T. C. Holmes (New York University, New York, NY). Human Kv1.5 in pBK was from Tamkun's laboratory. Kv1.3 and Kv1.5 were subcloned into pEYFP-C1 and pECFP-C1 (Clontech). The constructs were verified by sequencing. The Golgi (pECFP-Golgi) and ER (pDsRed-ER) markers were obtained from Clontech.

HEK 293 cells were grown on gelatin-coated coverslips in Dulbecco's modified Eagle's medium containing 10% fetal bovine serum. Transient transfection was performed using Lipofectamine 2000 (Invitrogen) at nearly 80% confluence. Twenty-four hours after transfection, the cells were washed in phosphate-buffered saline (PBS), fixed, and mounted with Aqua Poly/Mount from Polysciences, Inc. Murine bone marrow-derived macrophages from 6–10-week-old BALB/c mice (Charles River laboratories) were isolated and cultured as described elsewhere (7, 12, 19). Briefly, the animals were killed by cervical dislocation, and both femurs were dissected with the adherent tissue removed. The ends of bones were cut off, and the marrow tissue was flushed by irrigation with medium. The marrow plugs were passed through a 25-gauge needle for dispersion. The cells were cultured in plastic dishes (150 mm) in Dulbecco's modified Eagle's medium containing 20% fetal bovine serum and 30% L-cell-conditioned media as a source of macrophage-colony stimulating factor. The macrophages were obtained as a homogeneous population of adherent cells after 7 days culture and maintained at 37 °C in a humidified 5% CO_2 atmosphere. Bone marrow-derived macrophages were cultured in the absence or the presence of 100 ng/ml lipopolysaccharide (LPS) for 24 h. All of the animal handling was approved by the ethics committee of the University of Barcelona and was in accordance with European Union regulations.

Because lipid rafts are sensitive to cholesterol-modifying agents, in some experiments, transfected HEK cells were incubated in the presence or the absence of 2% methyl-β-cyclodextrin (MβCD) 1 h before raft isolation and confocal microscopy experiments (23, 24).

Immunostaining—Anti-transferrin receptor polyclonal, mouse anti-clathrin, and anti-caveolin polyclonal, which recognizes caveolin isoforms 1, 2, and 3, were from BD Transduction. Antiserum against the S1-S2 epitope of Kv1.5 was generated in the Philipson laboratory as previously described (25). Anti-Kv1.3, anti-Kv1.3 external epitope, and anti-Kv1.5 polyclonal antibodies were from Alomone. Alexa Fluor secondary antibodies were from Molecular Probes.

Transient transfected cells fixed with 4% paraformaldehyde in PBS for 10 min were further permeabilized with 0.5% CHAPS/PBS for 15 min. After 30 min of incubation with blocking solution (10% goat serum, 5% nonfat dry milk, PBS), the cells were reacted with anti-caveolin polyclonal (1:250) in 10% goat serum, 0.5% CHAPS, PBS for 1 h. The cells were further incubated 45 min with Alexa Fluor antibody (1:500) in PBS. The experiments were performed at room temperature.

For antibody-induced patching experiments, gelatin-coated coverslips with nonfixed cells were incubated with the S1-S2 Kv1.5 antiserum or anti-Kv1.3 external epitope antibody (diluted 1:1000 and 1:200, respectively) in HEPES-based culture medium for 1 h at room temperature. The cells were washed in PBS and further incubated with Alexa 488 anti-rabbit (1:500). The cells were fixed in methanol for 2 min and further stained with anti-caveolin antibody. Alexa 594 anti-mouse was used for caveolin visualization.

Raft Isolation and Immunoisolation of Caveolae—Low density, Triton-insoluble complexes were isolated as previously described (23, 24, 26) from bone marrow-derived macrophages and HEK cells transient transfected with either Kv1.3-YFP or double transfected Kv1.3-YFP/Kv1.5-CFP. The cells were homogenized in 1 ml of 1% Triton X-100, and sucrose was added to a final concentration of 40%. A 5–30% linear sucrose gradient was layered on top and further centrifuged (39,000 rpm) for 20–22 h at 4 °C in a Beckman SW41 rotor. Gradient fractions (1 ml) were collected from the top and analyzed by Western blot. The relative expression was analyzed by using Phoretix software, and statistics analysis was performed by Student's *t* test.

Isolation of caveolae has been described previously (23). Following sucrose gradient sedimentation, floating membranes were collected and pooled. The samples were diluted with Mes-buffered saline (25 mM Mes, pH 6.5, 0.15 M NaCl) containing 0.05% Triton X-100 and precleared with 25 μl of protein A-Sepharose beads for 2 h at 4 °C with gentle mixing. The beads were then removed by centrifugation at 200 × *g* for 2 min at 4 °C. The sample was then incubated overnight with anti-caveolin polyclonal antibodies (5 ng/ml) at 4 °C with gentle mixing. Twenty-five μl of protein A-Sepharose was added to each sample for 2 h at 4 °C. The beads were removed by centrifugation at 200 × *g* for 2 min at 4 °C, washed three times in PBS, and resuspended in 50 μl of SDS sample buffer.

Confocal Imaging: FRET and FRAP—Acceptor photobleaching was used to measure the FRET. Fluorescent proteins from fixed cells were excited with the 458 and 514-nm lines using low excitation intensities and 475–495-nm band pass and >530-nm long pass emission filters, respectively. Subsequently YFP protein from half of the cell was bleached by using maximum laser power obtaining ~80% of acceptor intensity bleaching. After photobleaching, images of the donor and acceptor were taken. FRET efficiency was calculated as $[(F_{CFPafter} - F_{CFPbefore})/F_{CFPbefore}]\times100$, where $F_{CFPafter}$ is the fluorescence of donor after bleaching, and $F_{CFPbefore}$ is before bleaching. Loss of fluorescence caused by scans was corrected measuring CFP intensity in the non-bleached part of the cell. FRET values were expressed as the means and standard error of $n > 15$ cells for each group.

FRAP experiments were performed 1 day after transfection at room temperature. The dishes were replaced every 2 h. Time series were taken with one scan before bleaching, ~30 iterations of bleaching with 100% laser power of the 514-nm line, followed by 4.5-s interval scans of the bleached region with 1–4% of laser power. In each cell, three different membrane regions were bleached to reduce local variations. The experiments were performed with $n > 15$ cells/group. Fluorescence intensity was normalized to the prebleach intensity. Any loss of fluorescence during the recording was corrected with unbleached regions of the cell. The values were fitted to a non-linear regression equation, $F(t) = M[1 - \exp(-t/t_{½})]$, where F is the fluorescence intensity, M is the mobile fraction, and $t_{½}$ is the time constant. The data are shown as the means ± S.E. Statistical analysis was performed by Student's *t* test (GraphPad Prism™). The cells were examined with a 63× oil immersion objective on a Zeiss LSM510 and a Leica TCS SL laser scanning confocal microscope.

Electrophysiology—Whole cell currents were measured using the patch clamp technique. An EPC-9 (HEKA) with the appropriate software was used for data recording and analysis. The currents were filtered at 2.9 kHz. Series resistance compensation was always above 70%. Patch electrodes of 2–4 MOhms were fabricated in a P-97 puller (Sutter Instruments Co.) from borosilicate glass (outer diameter, 1.2 mm; inner diameter, 0.94 mm; Clark Electromedical Instruments Co.). The electrodes were filled with the following solution 120 mM KCl, 1 mM $CaCl_2$, 2 mM $MgCl_2$, 10 mM HEPES, 11 mM EGTA, 20 mM D-glucose, adjusted to pH 7.3 with KOH. The extracellular solution contained 120 mM NaCl, 5.4 mM KCl, 2 mM $CaCl_2$, 1 mM $MgCl_2$, 10 mM HEPES, 25 mM D-glucose, adjusted to pH 7.4 with NaOH. After establishing the whole cell configuration of the patch clamp technique, the cells were clamped to a holding potential of −60 mV. To evoke voltage-gated currents, all of the cells were stimulated with 200-ms square pulses ranging from −50 to +50 mV in 10-mV steps. All of the recordings were routinely subtracted for leak currents. Conductance *versus* test potential was calculated as previously described (12).

To block K^+ currents, Margatoxin (Alomone) was added to the external solution. Before the experiments, toxin was reconstituted to 10 μM in Tris buffer (0.1% bovine serum albumin, 100 mM NaCl, 10 mM Tris, pH 7.5). All of the recordings were made at room temperature (20–23 °C).

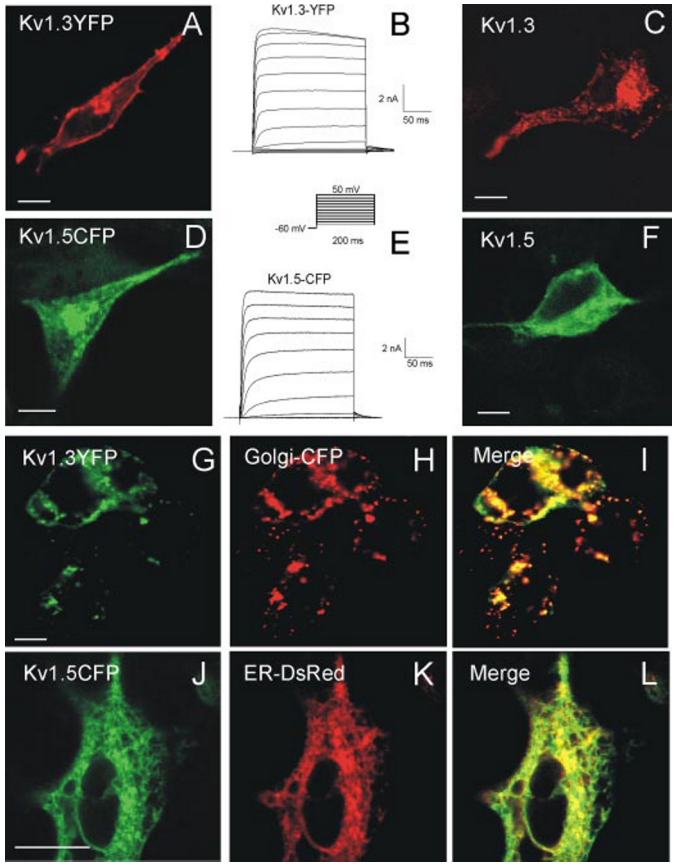

FIGURE 1. **Kv1.3-YFP and Kv1.5-CFP have distinct cellular distributions.** HEK cells were transient transfected with either wild type Kv1.3 (*C*) and Kv1.5 (*F*) or Kv1.3-YFP (*A* and *B*) and Kv1.5-CFP (*D* and *E*). Representative traces of K^+ currents from Kv1.3-YFP (*B*) and Kv1.5-CFP cells (*E*) are shown. The cells were held at −60 mV, and currents were elicited by depolarizing pulses in 10-mV steps (200 ms in duration) from −50 to +50 mV. *C*, immunolocalization of untagged Kv1.3. *F*, untagged Kv1.5. *G–I*, Kv1.3-YFP cotransfected with Golgi-CFP marker. *J–L*, Kv1.5-CFP cotransfected with DsRed-ER marker. *I* and *L*, merge panels show colocalization (*yellow*). The *bars* represent 10 μm.

RESULTS

Kv1.3 and Kv1.5 Localize to Different Intracellular Compartments—Kv1.3-YFP and Kv1.5-CFP constructs expressed in HEK cells (Fig. 1, *A* and *D*) were functional (Fig. 1, *B* and *E*). Although Kv1.3-YFP had good surface expression, Kv1.5-CFP showed intracellular retention. This was not due to the fluorescence tagging. Immunostaining experiments with cells express-

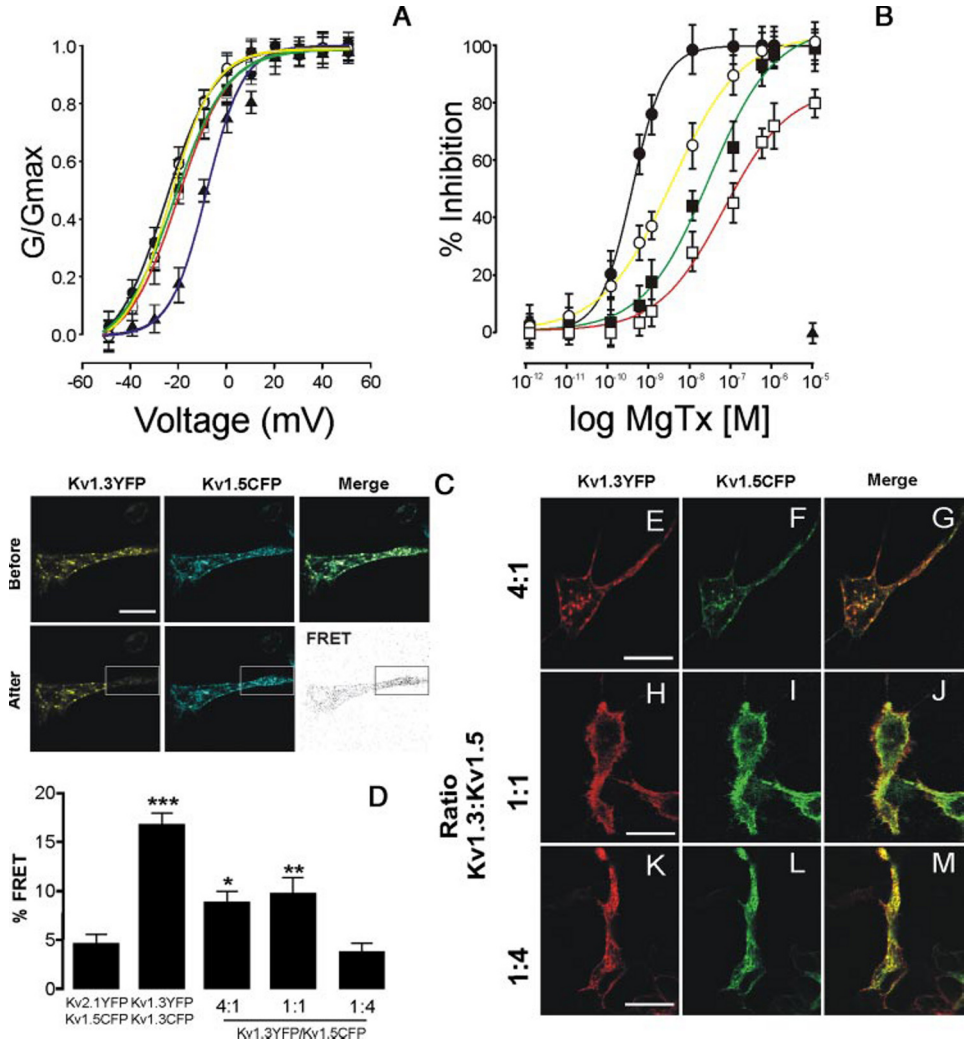

FIGURE 2. **Kv1.3 associates with Kv1.5, leading to biophysically and pharmacologically distinct channels.** HEK cells were doubly transfected with different ratios of Kv1.3-YFP and Kv1.5-CFP. *A*, plot of normalized conductance *versus* voltage of K^+ currents from HEK cells expressing different channel ratios. The pulse protocols are shown in Fig. 1. The conductance was normalized to the peak current at +50 mV. *B*, inhibition of the K^+ current by Margatoxin. The currents were evoked at +50 mV from a holding potential of −60 mV during a pulse potential of 200 ms. The percentage of inhibition was calculated by comparing the current at a given concentration of toxin *versus* that obtained in its absence. The values are the means ± S.E. The symbols and color lines are: Kv1.3-YFP (*black circles*, *black line*), Kv1.5-CFP (*closed triangle*, *blue line*), and the different Kv1.3-YFP/Kv1.5-CFP ratios 4:1 (*white circles*, *yellow line*), 1:1 (*black squares*, *green line*), and 1:4 (*white squares*, *red line*). *C*, representative FRET experiment. Panels show fluorescence signal of Kv1.3-YFP and Kv1.5-CFP (ratio 1:1) before and after photobleaching of the YFP region bounded by the *rectangle*. The *FRET panel* represents the difference of CFP fluorescence intensity after and before photobleaching. *D*, histogram shows FRET efficiency of different ratios of Kv1.3-YFP and Kv1.5-CFP. Negative control was performed with cells expressing Kv1.5-CFP and Kv2.1-YFP. Positive control was performed using cells expressing Kv1.3-CFP and Kv1.3-YFP. *, $p < 0.05$; **, $p < 0.01$; ***, $p < 0.001$ *versus* Kv2.1/Kv1.5 (Student's *t* test). *E–M*, HEK cells were doubly transfected with different ratios of Kv1.3-YFP (*red*) and Kv1.5-CFP (*green*). The merge panels show colocalization (*yellow*). Kv1.3 and Kv1.5 colocalized in HEK cells with 4:1 (*E–G*), 1:1 (*H–J*), and 1:4 (*K–M*) ratios. The *bars* represent 10 μm.

ing Kv1.3 and Kv1.5 wild type channels (Fig. 1, *C* and *F*) showed similar patterns.

Channel distribution was studied intracellularly. Coexpression of Kv1.5-CFP with an ER marker showed that this protein was mostly retained in this compartment (Fig. 1, *J–L*). Although Kv1.3-YFP did not colocalize with ER (data not shown), a Golgi signal was present in most of the intracellular vesicles (Fig. 1, *G–I*). This intracellular distribution was not a consequence of the presence of Golgi-CFP marker because expression of Kv1.3 alone gave similar results (supplemental Movie S1). Furthermore, living cells revealed dynamic traffic of Kv1.3 from the trans-Golgi network to cell membrane (supplemental Movie S2).

Kv1.3 and Kv1.5 Generate Functional Heterotetramers with Distinct Surface Expression—Different ratios of Kv1.3 and Kv1.5 generated biophysically and pharmacologically distinct channels (Fig. 2, *A* and *B*). K^+ currents were evoked in cells cotransfected with different ratios of Kv1.3 and Kv1.5. Steady state activation curves for Kv1.3, Kv1.5, and Kv1.3/Kv1.5 indicate that although increasing concentrations of Kv1.5 did not modify *k* slope values (11 ± 1, 7 ± 1, 9 ± 1, 11 ± 1, and 10 ± 1 for Kv1.3, Kv1.5, and 4:1, 1:1, and 1:4 Kv1.3/Kv1.5 ratios, respectively), half-activation voltages ($V_{½}$) shifted to depolarizing potentials (−15 ± 1, 2 ± 1, −14 ± 1, −11 ± 1, and −10 ± 1 for Kv1.3, Kv1.5, and 4:1, 1:1, and 1:4 Kv1.3/Kv1.5 ratios, respectively). Pharmacological experiments demonstrated that, unlike Kv1.5, Kv1.3, and hybrid Kv1.3/Kv1.5 channels were sensitive to Margatoxin. IC_{50} values were 0.3 ± 0.02, 3 ± 0.4, 25 ± 8, and 58 ± 17 nM for Kv1.3 and Kv1.3/Kv1.5 heteromers (4:1, 1:1, 1:4), respectively. These results support the idea that Kv1.5 coassembles with Kv1.3, thus generating multiple heterotetrameric channels.

FRET also demonstrated that Kv1.3 and Kv1.5 coassemble forming heteromers (Fig. 2, *C* and *D*). Although homotetrameric Kv1.3 channels, used as a positive control, gave ~17% FRET efficiency (Fig. 2*D*), cotransfection of YFP with CFP did not vary from 0% (data not shown). Kv2.1 does not associate with members of the Kv1 family (27). However, cotransfection of Kv1.5 and Kv2.1 gave <5% FRET efficiency. This energy transfer could be caused by the fixation step because both subunits, which are processed in ER, did not colocalize at the surface (data not shown). Low ratios of Kv1.5 (4:1, 1:1) were significantly different from negative controls, but FRET efficiencies were lower than those of Kv1.3. The FRET efficiency of Kv1.3/Kv1.5 (ratio 1:4) was <5%. There could be two reasons for this. First, the FRET efficiency was measured by changes in the CFP signal (supplemental Fig. S1), and the formation of Kv1.5-CFP homotetramers might mask

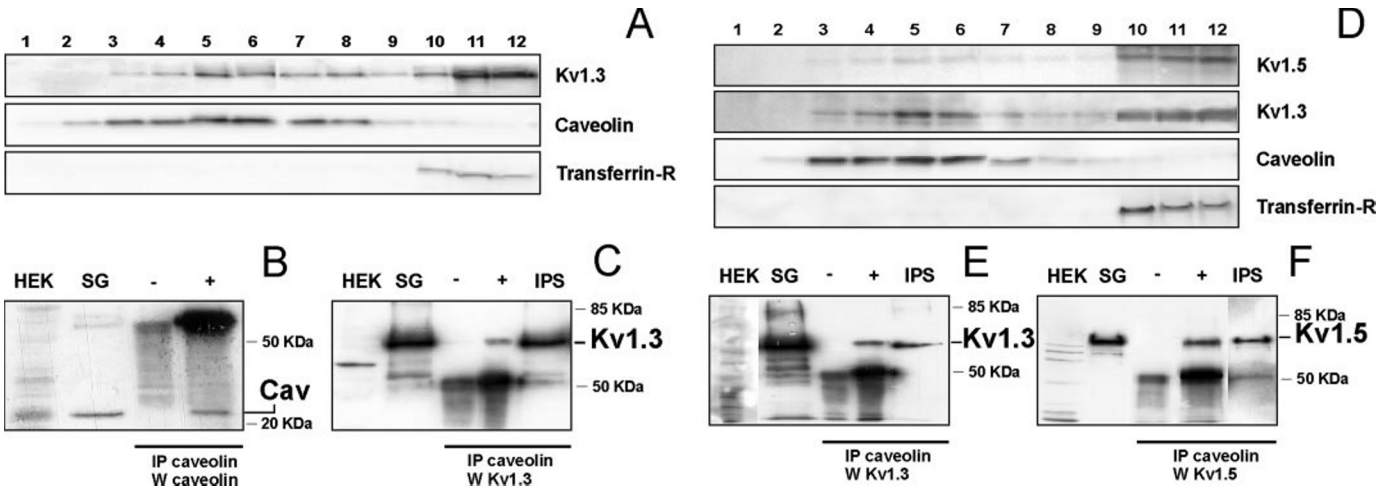

FIGURE 3. **Kv1.3 and Kv1.3/Kv1.5 heterotetramers target to lipid rafts.** Detergent-based isolation of lipid rafts. Sucrose density gradient centrifugation of 1% Triton X-100-solubilized extracts from cells, transfected with Kv1.3 alone (*A–C*) or doubly transfected with Kv1.3 and Kv1.5 (*D–F*), were analyzed by Western blot. While caveolin indicates low buoyancy rafts, transferrin receptor (*Transferrin-R*) distributes in nonfloating fractions. *B* and *C*, fractions 5 and 6 from *A* were immunoprecipitated (*IP*) with anti-caveolin antibody, and blots were immunoblotted (*W*) against caveolin (*B*) and Kv1.3 (*C*). *E* and *F*, fractions 5 and 6 from *D* were immunoprecipitated (*IP*) with anti-caveolin antibody, and blots were immunoblotted (*W*) against Kv1.3 (*E*) and Kv1.5 (*F*). *HEK*, membrane extracts from nontransfected HEK cells; *SG*, sucrose fractions number 5 and 6 as starting material; *IPS*, immunoprecipitated supernatant; −, immunoprecipitation in the absence of anti-caveolin antibody; +, immunoprecipitation in the presence of anti-caveolin antibody.

the analysis. In fact, the highest ratio of Kv1.5 (1:4) resulted in ~20% of current resistant to Margatoxin (see Fig. 2*B*). In addition, three donors and one acceptor in the complex might generate lower transfer efficiencies. Similar percentages were obtained with reciprocal Kv1.3-CFP and Kv1.5-YFP constructions (data not shown).

Kv1.3 traffic was influenced by the presence of Kv1.5. To determine whether the composition of heteromeric complexes governs the surface expression, different ratios of both subunits were transfected (Fig. 2, *E–M*). Both channels colocalized whatever the ratio used. However, increasing concentrations of Kv1.5 modified the traffic, ranging from homomeric Kv1.3 to resemble Kv1.5 channels. Although 4:1 (Fig. 2, *E–G*) and 1:1 (Fig. 2, *H–J*) Kv1.3/Kv1.5 ratios had surface expression, a 1:4 ratio presented high ER retention (Fig. 2, *K–M*) similar to Kv1.5 alone.

Kv1.3 and Kv1.5 Target to Lipid Rafts—Activation and apoptosis involve a specific surface location of Kv1.3 (28). Changes in this distribution, such as different lipid raft populations, determine different spatial regulations affecting the function (17, 18). Although Kv1.3 targets to lipid rafts, Kv1.5 localization is uncertain (16, 23, 29, 30). Therefore we wanted to study whether Kv1.3 and Kv1.3/Kv1.5 heteromers target to these domains. We carried out lipid raft extractions from HEK cells transfected with Kv1.3 (Fig. 3, *A–C*) and Kv1.3/Kv1.5 (ratio 1:1) (Fig. 3, *D–F*). In both cases, floating fractions contained Kv1.3. Kv1.5 was located in the same aliquots when cotransfected with Kv1.3 (Fig. 3*D*). Immunoprecipitation under nonsolubilizing conditions using Kv1.3 raft fractions (5 and 6) was performed with anti-caveolin antibody. Kv1.3 and Kv1.5 immunoprecipitated with caveolin in cells expressing Kv1.3 and Kv1.3/Kv1.5 (ratio 1:1) (Fig. 3, *C*, *E*, and *F*). Although Kv1.5 localized with caveolin direct interaction between the two proteins is debatable (23, 30). In this vein, we were unable to precipitate either Kv1.3 or Kv1.5 in HEK cells coexpressing Kv1.3 and Kv1.5 (ratio 1:4) (data not shown).

Lipid rafts are sensitive to cholesterol-modifying agents (23, 24, 26). Treatment of cells with 2% MβCD shifted the buoyancy of Kv1.3 and Kv1.5 containing rafts toward nonfloating fractions (Fig. 4, *A–D*) without altering the channel expression pattern (Fig. 4*E*). These results indicated that, in the absence of the cholesterol-binding drug, channels targeted to cholesterol-rich membrane domains. However, our data also suggested that the heterotetramer mainly targeted to different raft population. Thus, the heteromeric association modified the buoyancy of the proteins (Fig. 4, *A* and *B*). Although Kv1.3 and Kv1.5 located in low buoyancy fractions by 64 ± 5 and 19 ± 1%, respectively, their association shifted the floatability to 25 ± 2 and 26 ± 2%, respectively. In this context, although membrane patching experiments showed surface colocalization of Kv1.3 (Fig. 5, *A–C*) and Kv1.5 (Fig. 5, *D–F*) with caveolin, the latter was partial. This approach was unsuccessful with heterotetramers because neither anti-Kv1.5 nor anti-Kv1.3 antibodies recognized the complex.

Intracellular Kv1.3 distributed mostly in Golgi (see Fig. 1 and supplemental Movies S1 and S2), and caveolin-1 exhibited similar distributions (data not shown). Hence, we analyzed the presence of caveolin in Kv1.3-related Golgi vesicles. Caveolin was present in most of the Kv1.3 vesicles (Fig. 5, *G–I*). Kv1.3/Kv1.5 (ratio 1:1) channels also colocalized with intracellular caveolin (Fig. 5, *J–M*). This distribution was less robust than that observed for Kv1.3 and clearly deficient with high Kv1.5 (1:4 Kv1.3/Kv1.5) ratios (Fig. 5, *N–Q*). Kv1.5 alone produced similar results because channels were retained in ER. High Kv1.5 ratios relocalized hybrid channels out of caveolin vesicles. Therefore, a different composition of the heterotetramer modified the association with the caveolin traffic, which could impair the presence of channels in raft domains.

Kv1.5 Modifies Kv1.3 Mobility at the Cell Surface—The composition of raft microdomains is crucial for Kv1.3 activity, thereby modulating immune responses (17, 18, 28). To further

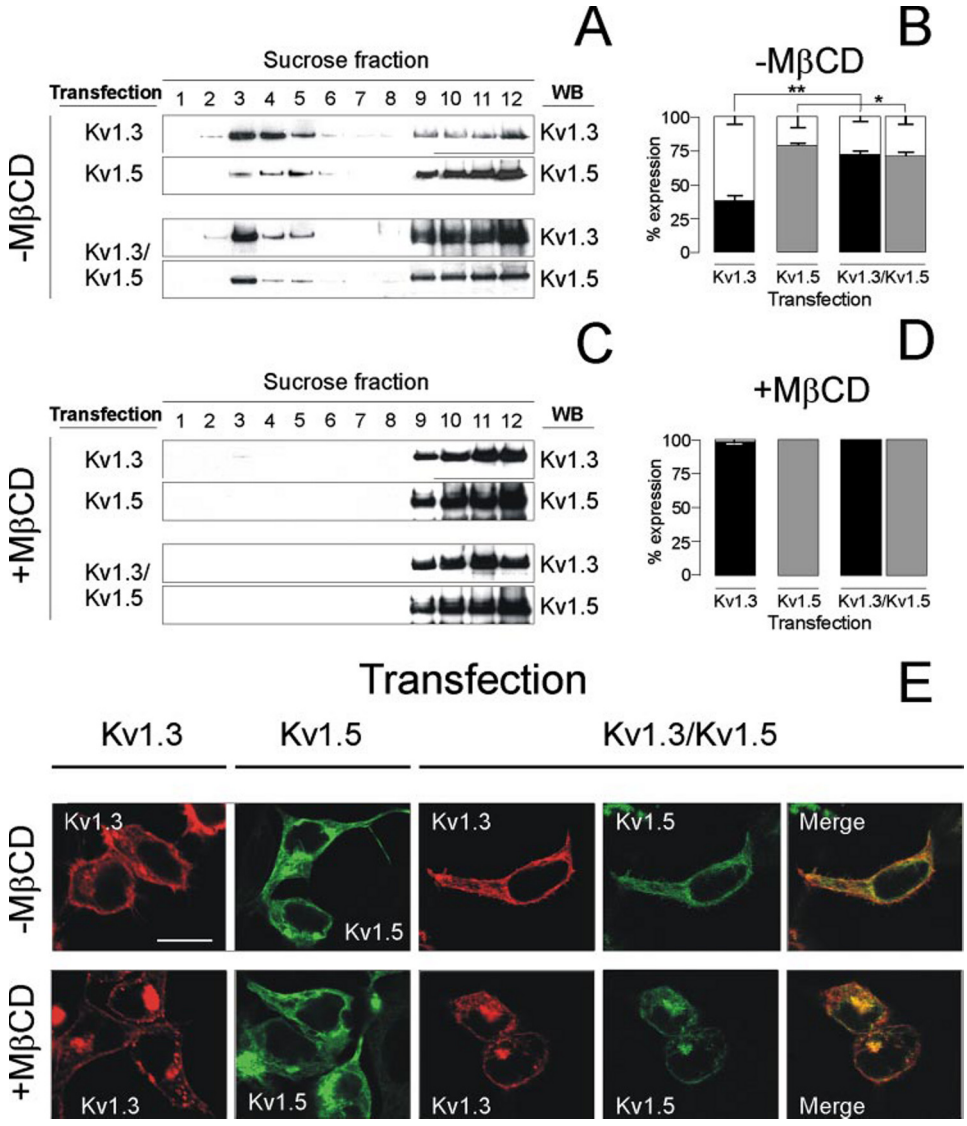

FIGURE 4. **Cholesterol depletion impairs Kv1.3, Kv1.5, and Kv1.3/Kv1.5 localization in lipid rafts.** HEK cells were treated with or without 2% MβCD 1 h before lipid raft extraction (*A–D*) and confocal microscopy studies (*E*). *A* and *C*, cells were transfected with Kv1.3, Kv1.5, and Kv1.3/Kv1.5 (ratio 1:1) and fractions immunoblotted (*WB*) against the channels. *B* and *D*, quantification of data from *A* and *C*. Relative abundance (%) of the protein expression located in floating (*white bar*) and nonfloating (*black bar*, Kv1.3; *gray bar*, Kv1.5) fractions. 100% represents the overall protein expression in all fractions. The values are the means ± S.E. of four independent experiments. *, $p < 0.05$; **, $p < 0.01$ (Student's *t* test). *A* and *B*, cells incubated without MβCD (−MβCD). *C* and *D*, cells incubated with MβCD (+MβCD). *E*, MβCD did not alter Kv1.3, Kv1.5, and Kv1.3/Kv1.5 expression patterns. The cells were transfected as described above and incubated in the absence (*top panels*, −MβCD) or the presence (*bottom panels*, +MβCD) of MβCD. HEK cells were transfected with Kv1.3-YFP (*red*), Kv1.5-CFP (*green*), and both (Kv1.3/Kv1.5). The merge panels show colocalization (*yellow*) in doubly transfected cells. The *bars* represent 10 μm.

investigate whether Kv1.3 homo- and Kv1.3/Kv1.5 heterotetramers target to different raft domains, we performed FRAP experiments (Fig. 6). Fluorescence recovery within membrane regions was monitored until a steady state was achieved (supplemental Movie S3). Mobile fractions were similar (55 ± 1 and 57 ± 1% for Kv1.3 and Kv1.3/Kv1.5 (1:1) respectively), but the time constant ($t_{½}$) of the heteromer exhibited higher lateral mobility (45.7 ± 1.4 s and 33.2 ± 1.3 s for Kv1.3 and Kv1.3/Kv1.5 (1:1), respectively, $p <$ 0.001). These results were not a consequence of a turnover from the trans-Golgi network (supplemental Movie S4). Such experiments were not possible with Kv1.5 and Kv1.3/Kv1.5 (ratio 1:4), because, as shown in Figs. 1 and 2, channels were mostly ER-retained. Our results indicate that Kv1.5 targets Kv1.3 to different raft populations with higher mobility.

Activation of Macrophages Relocalizes Kv1.5 in Lipid Rafts—The localization of Kv1.5 in lipid rafts is under debate, and the association with caveolin is one of the main issues (23, 24, 30). We have demonstrated that Kv1.5 associates with Kv1.3 generating multiple functional channels that target to distinct raft microdomains. This is important in leukocytes where Kv1.3 and rafts concentrate at the immunological synapse, and raft composition regulates Kv1.3-related cellular functions (16–18, 28). Unlike T-lymphocytes, macrophages express Kv1.3 and Kv1.5 channels (7, 12, 13, 19). Raft extractions showed that, although Kv1.3 colocalized partially with caveolin (12 ± 2%), Kv1.5 did not target to lipid rafts (Fig. 7). Therefore, unlike Kv1.3 homomers, Kv1.3/Kv1.5 hybrid channels localize in nonfloating fractions. Macrophage activation selectively induced Kv1.3, which increases the Kv1.3/Kv1.5 ratio in the heteromeric channel (12, 13, 19), and also augmented caveolin in the same fractions. Rafts extractions from LPS-activated macrophages showed that more Kv1.3 colocalized with caveolin and Kv1.5 appeared in low buoyant density fractions (40 ± 3 and 10 ± 1% for Kv1.3 and Kv1.5, respectively). Our results indicate that different physiological mechanisms govern Kv1.3 and Kv1.5 locations in rafts, which lead to different spatial regulation of Kv1.3/Kv1.5 heterotetramers.

DISCUSSION

Traffic and subcellular localization regulate ion channel activities which are essential to understanding their role (15, 31). Kv channels are either homo- or heterotetramers, and different structures modulate surface expression leading to another mechanism regulating channel activity. This has been suggested for neurons, where Kv1.1, Kv1.2, and Kv1.4 heteromeric channels show different traffic and surface expression (8). Immune system cells express a unique subset of Kv channels, with Kv1.3 being the major isoform (1, 2). Kv control rest-

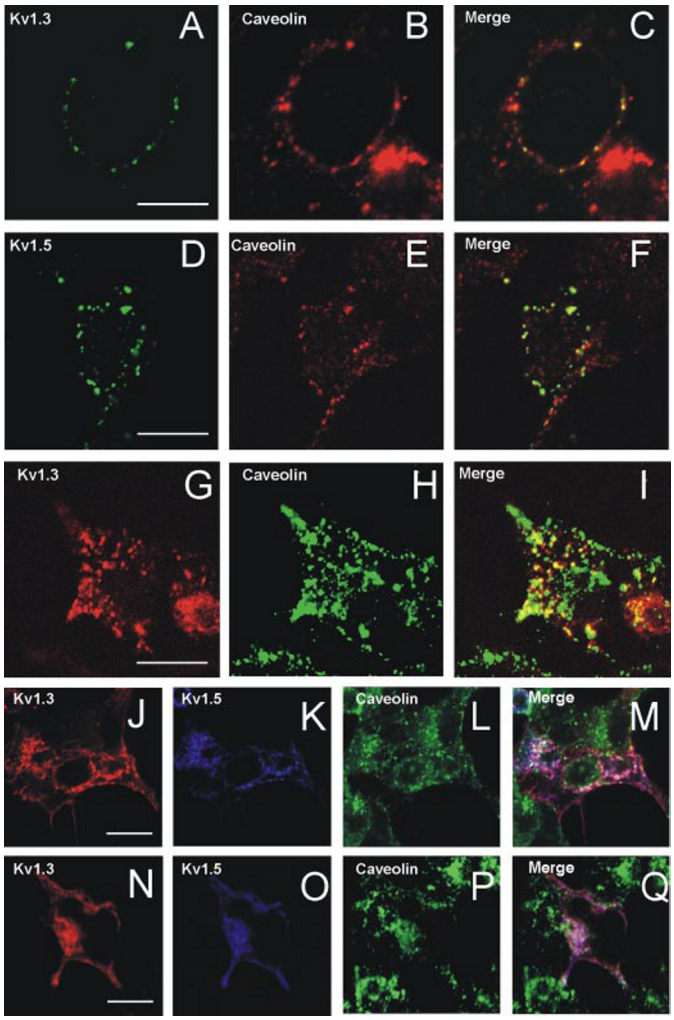

FIGURE 5. **Kv1.3 and Kv1.5 colocalize with caveolae in HEK cells.** *A* and *D*, cells expressing Kv1.3 and Kv1.5 patched with their respective antibody against external epitope. *B* and *E*, caveolin. *C* and *F*, merge panels showed colocalization (*yellow*). *G–I*, intracellular Kv1.3 traffics with caveolin. *G*, Kv1.3-YFP; *H*, caveolin; *I*, colocalization (*yellow*). Hybrid Kv1.3/Kv1.5 channels (ratio 4:1, *J–M*) but not ratio 1:4 (*N–Q*) colocalized with intracellular caveolin. *J* and *N*, Kv1.3-YFP. *K* and *O*, Kv1.5-CFP. *L* and *P*, Caveolin. *M* and *Q*, colocalization between Kv1.3 and Kv1.5 (*pink*) or triple colocalization with caveolin (*white*). The *bars* represent 10 μm.

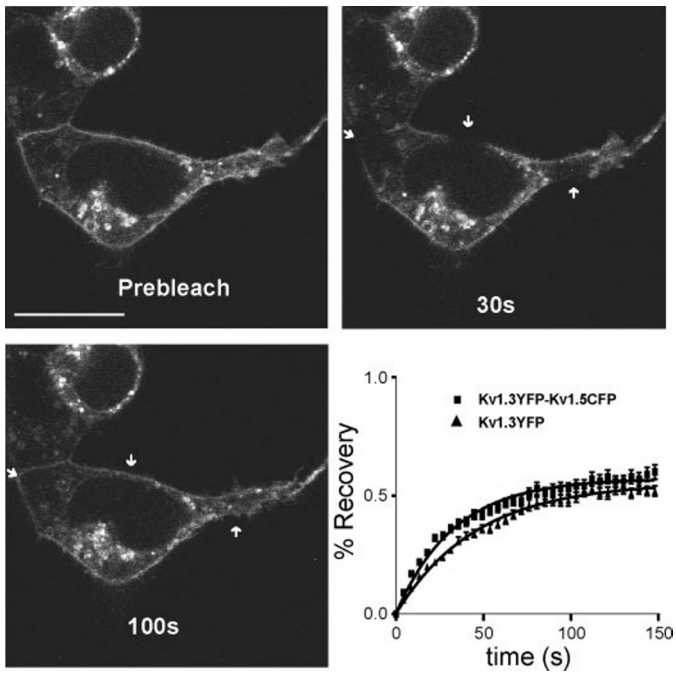

FIGURE 6. **FRAP of Kv1.3 and heterotetramer Kv1.3/Kv1.5.** FRAP experiments monitored YFP intensity after bleaching for 150 s. Representative images of Kv1.3-YFP at different times are shown. The *arrows* indicate regions of analysis. The *bar* represents 10 μm. The *graph* represents the regression analysis of data from Kv1.3 and heterotetramer Kv1.3/Kv1.5.

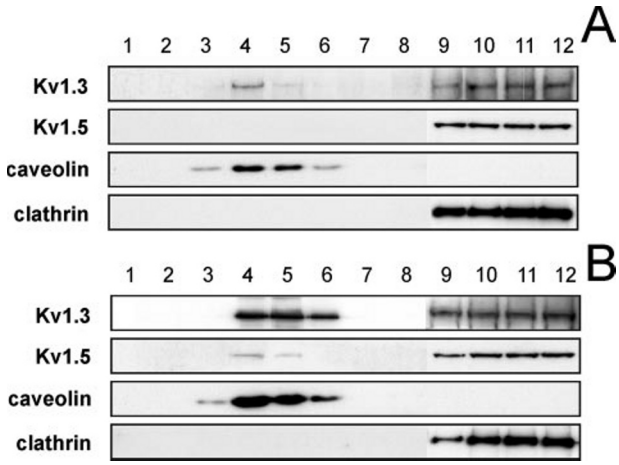

FIGURE 7. **Activation of macrophages targets Kv1.5 back to lipid rafts.** Detergent-based isolation of lipid rafts from bone marrow derived macrophages cultured in the absence (*A*) or the presence (*B*) of 100 ng/ml LPS. Sucrose density gradient fractions were analyzed by Western blot. Although caveolin localized low buoyancy raft fractions, clathrin marked nonfloating fractions. LPS increased the relative abundance of Kv1.3 (12 $\pm$ 2 and 40 $\pm$ 3%, for control and LPS-treated cells, respectively; $p < 0.01$, Student's *t* test) and shifted Kv1.5 to low buoyancy rafts (10 $\pm$ 1% in LPS-treated cells) in macrophages. The values are the means $\pm$ S.E. of four independent experiments.

ing membrane potential and are involved in activation and proliferation. Kv1.3 localizes in the immunological synapse and targets to different raft domains upon activation and apoptosis in T-cells (16, 28). In addition to Kv1.3, Kv1.5 is also expressed in the myeloid lineage (19–21) and exerts important physiological and pharmacological consequences in macrophages (13, 20, 22). Here we studied whether the association of Kv1.3 and Kv1.5 influences traffic and targeting. These determinants affect the expression and functional properties of the channels and contribute to the diversity of K^+ channels in leukocytes.

Kv1.3 has good surface expression. However, Kv1.5 shows less robust membrane localization, being retained in ER (23, 32, 33). Differential surface location and traffic have been described for several Kv1 channels. Although Kv1.4 shows strong plasma membrane expression, Kv1.1 and Kv1.2 are retained in ER (8, 9). Folding and assembly efficiencies, controlled by chaperon-like proteins such as calnexin or β subunits, could determine this variation (31, 34). In addition, several ER retention signals within the pore and C- and N-terminal domains determine traffic and surface expression (29). Although V*XX*SL in the C terminus is considered a strong ER export motif, neither Kv1.3 nor Kv1.5 shares this element. In contrast, Kv1.3 and Kv1.5 possess basic intracellular motifs (R*X*R and RR) near the T1 tetramerization domain that serve as ER retention signals (35). Positive and negative determinants have also been reported within the pore (31, 36). An external

proline in the pore, which is involved in Kv1.4-mediated ER export (Pro^{505}), is present in Kv1.3 (Pro^{374}) but is not conserved in Kv1.5 (Gln^{453}). Many underlying mechanisms must be involved in Kv location. Although KChIP2 (Kv channel interacting protein 2) enhances the membrane surface expression of Kv4.2, it reduces Kv1.5 forward trafficking from the ER (37). Our results implicate other elements, which need further research.

Kv1.3 coassembles with Kv1.5 forming functional heterotetrameric complexes, and the stoichiometry determines the traffic. Increasing concentrations of Kv1.5 impair Kv1.3 surface expression and modulate Kv activity. Thus, the heterotetramer activity results from a mixture of characteristics of the isoforms that comprise the channel. Consequently, differential expression of Kv1.3 and Kv1.5 changes the number of channels at the surface, modifying the membrane excitability and signaling.

Lipid raft sublocalization regulates ion channels providing compartmentalization where signal transduction pathways converge. For instance, Kv1.3 targets to different rafts upon activation and apoptosis in lymphocytes (16, 28). Disruption of these domains alters channel activity, and raft association seems to be dynamic (15, 17, 18, 29, 38). Scaffolding proteins like membrane-associated guanylate kinases are involved in the K^+ channel association with raft domains. This is the case of PSD-95 for Kv1.4 or SAP97 for Kv1.5 (29, 38, 39). In addition, Kv1.5 targets to caveolae without an apparent physical association (23), but it forms macromolecular complexes with SAP97 and caveolin-3 (29). Our results indicate that Kv1.5 localization in caveolae could be partial and strongly dependent on scaffolding and heterotetrameric associations. In fact, caveolin regulates Kv1.5 trafficking to cholesterol-rich membrane microdomains in thyroid cells but not in cardiomyocytes (24, 32). Although, we found that Kv1.3 and Kv1.5 localized in lipid rafts, Kv1.5-containing channels in macrophages mistargeted these domains. However, this may be counteracted by macrophage activation, which accumulates caveolin and increases the Kv1.3/Kv1.5 ratio (12, 13, 19). Similarly, Kv1.3 association shifts more Kv1.5 protein to low buoyancy rafts in HEK cells. These results indicate that different mechanisms govern Kv1.3 and Kv1.5 targeting to rafts altering the traffic and localization of hybrids.

In addition to Kv1.3 and Kv1.5, other Kv such as Kv1.4 and Kv2.1 also target to distinct surface microdomains (26, 40). Kv2.1 is retained within dynamic surface microdomains, but neither distribution nor mobility changes following cholesterol depletion (40, 41). Kv1.3 mobility is higher than for Kv1.4 and Kv2.1, and it is further increased by cyclodextrin (40). Kv1.3/Kv1.5 heteromer lateral mobility is even higher than that of Kv1.3, indicating that Kv1.5 changes the spatial regulation of Kv1.3. Macrophages do not express Kv1.5 homomeric channels (12, 13, 19), demonstrating that, unlike Kv1.3, hybrids Kv1.3/Kv1.5 do not colocalize in floating fractions. However, upon physiological stimuli, which increases the Kv1.3/Kv1.5 ratio (12, 13), channels relocalized in rafts.

To what extent our results explain the role of Kv1.3 in the cell signaling is not yet clear. Heteromeric structures, located in distinct surface microdomains, may respond differentially upon kinase activation. Kv1.3 and Kv1.5 are regulated by signaling molecules, such as PKC, PKA, and tyrosine kinases, which are localized in caveolar and noncaveolar microdomains (4, 5, 42). In addition, kinases are tightly modulated by distinct raft compositions (43, 44). PKA and PKC colocalize with caveolin-1 and cholesterol depletion regulates PKA and Kv1.3 (17, 44, 45). Interestingly, tyrosine phosphorylation of Kv1.3 suppresses currents and targeting of the channel to ceramide enriched platforms (5, 18). In microglia, where Kv1.5 controls distinct functions (20), transforming growth factor-β enhances Kv1.3 independently of PKA, PKC, tyrosine kinases, and mitogen-activated protein kinase extracellular signal-regulated kinase (ERK) (46). It is tempting to speculate that this deactivation is a consequence of a Kv1.3/Kv1.5 channel mistargeting to rafts in brain macrophages. Different phosphorylation mechanisms are also mediated by distinct membrane surface locations. Although PKA-mediated phosphorylation is related to the caveolae pathway, G protein-coupled receptor kinases mediate phosphorylation mainly in clathrin-coated pits (47). However, although ligand-dependent phosphorylation and internalization of epidermal growth factor receptor is via clathrin-coated pits, some phosphorylation of epidermal growth factor receptor localizes in caveolar lipid rafts (48, 49). This would agree with epidermal growth factor-mediated inhibition of Kv1.3 currents (5). In this scenario, caveolae control the spatial and temporal pattern of intracellular Ca^{2+} signaling (50) in which the localization of Kv1.3/Kv1.5 heteromeric channels plays a pivotal role, fine tuning the cellular responses. In fact, LPS-induced activation, which selectively accumulates more Kv1.3 in the Kv1.3/Kv1.5 channel (12, 13, 19), targets heterotetramers back to rafts.

In summary, Kv1.3 traffic, targeting, and activity are dramatically changed by the presence of Kv1.5. These two isoforms are coexpressed in the myeloid lineage of the immune system and play a crucial role in controlling the immunological response. Therefore, our results further the understanding of how voltage-dependent K^+ channels are involved in leukocyte physiology and open a new variable considering the use of Kv1.3 as a pharmacological target.

Acknowledgment—The editorial assistance of the Language Advisory Service from the University of Barcelona is acknowledged.

REFERENCES

1. Wulff, H., Beeton, C., and Chandy, K. G. (2003) *Curr. Opin. Drug. Discov. Dev.* **6,** 640–647
2. Beeton, C., and Chandy, K. G. (2005) *Neuroscientist* **11,** 550–562
3. Payet, M. D., and Dupuis, G. (1992) *J. Biol. Chem.* **267,** 18270–18273
4. Martel, J., Dupuis, G., Deschenes, P., and Payet, M. D. (1998) *J. Membr. Biol.* **161,** 183–196
5. Holmes, T. C., Fadool, D. A., and Levitan, I. B. (1996) *J. Neurosci.* **16,** 1581–1590
6. McCormack, T., McCormack, K., Nadal, M. S., Vieira, E., Ozaita, A., and Rudy, B. (1999) *J. Biol. Chem.* **274,** 20123–20126
7. Vicente, R., Escalada, A., Soler, C., Grande, M., Celada, A., Tamkun, M. M., Solsona, C., and Felipe, A. (2005) *J. Immunol.* **174,** 4736–4744
8. Manganas, L. N., and Trimmer, J. S. (2000) *J. Biol. Chem.* **275,** 29685–29693
9. Zhu, J., Watanabe, I., Gomez, B., and Thornhill, W. B. (2003) *J. Biol. Chem.* **278,** 25558–25567
10. Coleman, S. K., Newcombe, J., Pryke, J., and Dolly, J. O. (1999) *J. Neuro-*

chem. **73,** 849–858
11. Koch, R. O., Wanner, S. G., Koschak, A., Hanner, M., Schwarzer, C., Kaczorowski, G. J., Slaughter, R. S., Garcia, M. L., and Knaus, H. G. (1997) *J. Biol. Chem.* **272,** 27577–27581
12. Vicente, R., Escalada, A., Villalonga, N., Texido, L., Roura-Ferrer, M., Martin-Satue, M., Lopez-Iglesias, C., Soler, C., Solsona, C., Tamkun, M. M., and Felipe, A. (2006) *J. Biol. Chem.* **281,** 37675–37685
13. Villalonga, N., Escalada, A., Vicente, R., Sanchez-Tillo, E., Celada, A., Solsona, C., and Felipe, A. (2007) *Biochem. Biophys. Res. Commun.* **352,** 913–918
14. Schlegel, A., Volonte, D., Engelman, J. A., Galbiati, F., Mehta, P., Zhang, X. L., Scherer, P. E., and Lisanti, M. P. (1998) *Cell Signal.* **10,** 457–463
15. Martens, J. R., O'Connell, K., and Tamkun, M. (2004) *Trends Pharmacol. Sci.* **25,** 16–21
16. Panyi, G., Vamosi, G., Bacso, Z., Bagdany, M., Bodnar, A., Varga, Z., Gaspar, R., Matyus, L., and Damjanovich, S. (2004) *Proc. Natl. Acad. Sci. U. S. A.* **101,** 1285–1290
17. Hajdu, P., Varga, Z., Pieri, C., Panyi, G., and Gaspar, R., Jr. (2003) *Pflügers Arch. Eur. J. Physiol.* **445,** 674–682
18. Bock, J., Szabo, I., Gamper, N., Adams, C., and Gulbins, E. (2003) *Biochem. Biophys. Res. Commun.* **305,** 890–897
19. Vicente, R., Escalada, A., Coma, M., Fuster, G., Sanchez-Tillo, E., Lopez-Iglesias, C., Soler, C., Solsona, C., Celada, A., and Felipe, A. (2003) *J. Biol. Chem.* **278,** 46307–46320
20. Pannasch, U., Farber, K., Nolte, C., Blonski, M., Yan Chiu, S., Messing, A., and Kettenmann, H. (2006) *Mol. Cell Neurosci.* **33,** 401–411
21. Mullen, K. M., Rozycka, M., Rus, H., Hu, L., Cudrici, C., Zafranskaia, E., Pennington, M. W., Johns, D. C., Judge, S. I., and Calabresi, P. A. (2006) *Ann. Neurol.* **60,** 118–127
22. Park, S. A., Lee, Y. C., Ma, T. Z., Park, J. A., Han, M. K., Lee, H. H., Kim, H. G., and Kwak, Y. G. (2006) *Biochem. Biophys. Res. Commun.* **346,** 567–571
23. Martens, J. R., Sakamoto, N., Sullivan, S. A., Grobaski, T. D., and Tamkun, M. M. (2001) *J. Biol. Chem.* **276,** 8409–8414
24. McEwen, D. P., Li, Q., Jackson, S., Jenkins, P. M., and Martens, J. R. (2007) *Mol Pharmacol.* 10.1124/mol.107.042093
25. Philipson, L. H., Malayev, A., Kuznetsov, A., Chang, C., and Nelson, D. J. (1993) *Biochim. Biophys. Acta* **1153,** 111–121
26. Martens, J. R., Navarro-Polanco, R., Coppock, E. A., Nishiyama, A., Parshley, L., Grobaski, T. D., and Tamkun, M. M. (2000) *J. Biol. Chem.* **275,** 7443–7446
27. Lee, T. E., Philipson, L. H., Kuznetsov, A., and Nelson, D. J. (1994) *Biophys. J.* **66,** 667–673
28. Szabo, I., Adams, C., and Gulbins, E. (2004) *Pflügers Arch. Eur. J. Physiol.* **448,** 304–312
29. Folco, E. J., Liu, G. X., and Koren, G. (2004) *Am. J. Physiol.* **287,** H681–H690
30. Eldstrom, J., Van Wagoner, D. R., Moore, E. D., and Fedida, D. (2006) *FEBS Lett.* **580,** 6039–6046
31. Misonou, H., and Trimmer, J. S. (2004) *Crit. Rev. Biochem. Mol. Biol.* **39,** 125–145
32. Eldstrom, J., Doerksen, K. W., Steele, D. F., and Fedida, D. (2002) *FEBS Lett.* **531,** 529–537
33. Cogolludo, A., Moreno, L., Lodi, F., Frazziano, G., Cobeno, L., Tamargo, J., and Perez-Vizcaino, F. (2006) *Circ. Res.* **98,** 931–938
34. Manganas, L. N., and Trimmer, J. S. (2004) *Biochem. Biophys. Res. Commun.* **322,** 577–584
35. Colley, B. S., Biju, K. C., Visegrady, A., Campbell, S., and Fadool, D. A. (2007) *Neuroscience* **144,** 531–546
36. Manganas, L. N., Wang, Q., Scannevin, R. H., Antonucci, D. E., Rhodes, K. J., and Trimmer, J. S. (2001) *Proc. Natl. Acad. Sci. U. S. A.* **98,** 14055–14059
37. Li, H., Guo, W., Mellor, R. L., and Nerbonne, J. M. (2005) *J. Mol. Cell Cardiol.* **39,** 121–132
38. Pottosin, I. I., Valencia-Cruz, G., Bonales-Alatorre, E., Shabala, S. N., and Dobrovinskaya, O. R. (2007) *Pflügers Arch. Eur. J. Physiol.* **454,** 235–244
39. Wong, W., and Schlichter, L. C. (2004) *J. Biol. Chem.* **279,** 444–452
40. O'Connell, K. M., and Tamkun, M. M. (2005) *J. Cell Sci.* **118,** 2155–2166
41. O'Connell, K. M., Rolig, A. S., Whitesell, J. D., and Tamkun, M. M. (2006) *J. Neurosci.* **26,** 9609–9618
42. Kwak, Y. G., Hu, N., Wei, J., George, A. L., Jr., Grobaski, T. D., Tamkun, M. M., and Murray, K. T. (1999) *J. Biol. Chem.* **274,** 13928–13932
43. Prevostel, C., Alice, V., Joubert, D., and Parker, P. J. (2000) *J. Cell Sci.* **113,** 2575–2584
44. El-Yazbi, A. F., Cho, W. J., Schulz, R., and Daniel, E. E. (2006) *Am. J. Physiol.* **291,** G1020–G1030
45. Rybin, V. O., Xu, X., and Steinberg, S. F. (1999) *Circ. Res.* **84,** 980–988
46. Schilling, T., and Eder, C. (2003) *Pflügers Arch. Eur. J. Physiol.* **447,** 312–315
47. Rapacciuolo, A., Suvarna, S., Barki-Harrington, L., Luttrell, L. M., Cong, M., Lefkowitz, R. J., and Rockman, H. A. (2003) *J. Biol. Chem.* **278,** 35403–35411
48. Huang, F., Khvorova, A., Marshall, W., and Sorkin, A. (2004) *J. Biol. Chem.* **279,** 16657–16661
49. Liu, Y. T., Song, L., and Templeton, D. M. (2007) *J. Cell. Physiol.* **211,** 205–212
50. Isshiki, M., and Anderson, R. G. (1999) *Cell Calcium* **26,** 201–208